Check for updates

ChemSusChem

Chemistry–Sustainability–Energy–Materials

Chemistry Europe

European Chemical Societies Publishing

Accepted Article

Title: Upcycling Commodity Styrofoam into Redox Polymer-based Electrodes

Authors: Algin Biying Oh, Sabrina Trano, Yi Jie Eng, Gabriele Lingua, Haritz Sardon, David Mecerreyes, and Julian M. W. Chan

This manuscript has been accepted after peer review and appears as an Accepted Article online prior to editing, proofing, and formal publication of the final Version of Record (VoR). The VoR will be published online in Early View as soon as possible and may be different to this Accepted Article as a result of editing. Readers should obtain the VoR from the journal website shown below when it is published to ensure accuracy of information. The authors are responsible for the content of this Accepted Article.

To be cited as: *ChemSusChem* **2025**, e202500092

Link to VoR: https://doi.org/10.1002/cssc.202500092

WILEY VCH

1864564x, ja, Downloaded from https://chemistry-europe.onlinelibrary.wiley.com/doi/10.1002/cssc.202500092 by A*Star Research Entities, Wiley Online Library on [19/03/2025]. See the Terms and Conditions (https://onlinelibrary.wiley.com/terms-and-conditions) on Wiley Online Library for rules of use; OA articles are governed by the applicable Creative Commons License

Accepted Manuscript

Upcycling Commodity Styrofoam into Redox Polymer-based Electrodes

Algin Oh Biying,[a†] Sabrina Trano,[d†] Yi Jie Eng,[a] Gabriele Lingua,[b] Haritz Sardon,[b] David Mecerreyes,*[b,c] Julian M. W. Chan*[a]

[a] Institute of Sustainability for Chemicals, Energy and Environment (ISCE^2),

Agency for Science, Technology and Research (A*STAR),

1 Pesek Road, Jurong Island, Singapore 627833,

Republic of Singapore

*E-mail: julian_chan@isce2.a-star.edu.sg

[b] POLYMAT University of the Basque Country UPV/EHU,

Avenida Tolosa 72, 20018 Donostia-San Sebastián, Spain

[c] Ikerbasque, Basque Foundation for Science,

Maria Diaz de Haro 3, E–48011 Bilbao, Spain

*E-mail: david.mecerreyes@ehu.es

[d] Department of Applied Science and Technology

Politecnico di Torino, Corso Duca degli Abruzzi 24, 10129 Torino (Italy)

[†] These authors contributed equally to this work.

This article is protected by copyright. All rights reserved.

1864564x, ja, Downloaded from https://chemistry-europe.onlinelibrary.wiley.com/doi/10.1002/cssc.202500092 by A*Star Research Entities, Wiley Online Library on [19/03/2025]. See the Terms and Conditions (https://onlinelibrary.wiley.com/terms-and-conditions) on Wiley Online Library for rules of use; OA articles are governed by the applicable Creative Commons License

Accepted Manuscript

ABSTRACT

Commodity polystyrene from styrofoam food boxes was chemically transformed into redox-active organic polymers via a two-step functionalization sequence. In the first step, controlled chloromethylation of the pendent phenyl rings was used to functionalize 30–50% of the polymer chain. The degree of functionalization could be tuned by simply varying the reaction time (1–3 h). Next, phenothiazine or nitroxide radical moieties were introduced via nucleophilic displacement of the benzylic chlorides to afford polymers with redox-active pendent sidechains. These phenothiazine and TEMPO-functionalized polymers were then characterized electrochemically to demonstrate their redox properties and evaluate their performance as battery electrodes. Overall, this process serves as proof-of-concept for the rapid conversion of consumer-grade styrofoam into redox-active polymers with the potential to serve as metal-free electrodes in organic batteries.

This article is protected by copyright. All rights reserved.

1864564x, ja, Downloaded from https://chemistry-europe.onlinelibrary.wiley.com/doi/10.1002/cssc.202500092 by A*Star Research Entities, Wiley Online Library on [19/03/2025]. See the Terms and Conditions (https://onlinelibrary.wiley.com/terms-and-conditions) on Wiley Online Library for rules of use; OA articles are governed by the applicable Creative Commons License

Accepted Manuscript

INTRODUCTION

As a commodity plastic, polystyrene (PS) is one of the least frequently recycled (i.e., recycling rate of 0.9%) polymers and also one of the slowest to degrade in the environment.[1] In particular, expanded PS (or styrofoam) tends to be ineligible for recycling as its low density and large bulk makes it uneconomical to do so.[2] As a consequence, postconsumer styrofoam waste usually ends up in landfills, oceans, or the incinerator, none of which are environmentally friendly. In the quest for more palatable alternatives, researchers have explored new ways to chemically convert commodity PS into diverse functional materials via postpolymerization functionalization, but the overall efforts in this subarea remain somewhat sparse.[3-11] Compared to other common plastics such as polyethylene or polypropylene, PS is unique in that it contains useful benzene rings that lend themselves to various types of aromatic chemistry and can thus act as chemical handles for postpolymerization modification. However, in the majority of previous work on PS functionalization, only pure samples of commercial and laboratory-synthesized PS have been employed as the starting material,[3-8] as opposed to actual consumer PS items that usually come with impurities and/or additives. Thus, we have been interested in exploring robust chemistry that enable the rapid and controllable synthesis of custom functional materials from everyday styrofoam items.[9] In the present study, we sought to leverage simple and non-sensitive chemistries to upcycle commodity PS items into redox-active polymers that may serve as electrodes in rechargeable organic batteries.

Given the ever-increasing global demand for energy, along with the rising popularity of electric vehicles, consumer electronic devices, and energy storage systems, the pursuit of superior next-generation battery technologies continues to be one of the most active areas of research across multiple scientific disciplines.[12-14] In general, contemporary batteries (e.g., commercial lithium-ion batteries) rely overwhelmingly on conventional inorganic materials, e.g., lithium cobalt oxide and lithium iron phosphate as cathode materials.[15-17] Aside from the

This article is protected by copyright. All rights reserved.

problem of lithium and some transition metals being not very earth-abundant, the challenges and expense associated with recycling such batteries can also be significant.[18] Therefore, the search for alternative and more sustainable electrode materials now represents an area of considerable academic interest as well as a critical need in the rechargeable battery industry.

One class of materials that has been extensively studied over the past decade to fill this gap are the redox-active organic molecules/polymers. These organic materials represent promising candidates for electrode materials in rechargeable batteries because of inherent advantages such as higher elemental abundance (e.g., C, H, N, S), low cost, and potential for greater sustainability, tunability and mechanical flexibility.[19–25] Compared to currently used inorganic materials, organic materials show shortcomings which include poorer cyclability and stability as well as generally lower conductivities and energy densities.[22] Some organic materials may also exhibit appreciable solubility in organic electrolytes/solvents, resulting in leaching of the electrode material over time. Nonetheless, organic redox polymers offer the possibility of producing light-weight, potentially recyclable, and environmentally benign all-organic batteries that are completely free of heavy metals. Selected examples of organic functional groups and polymers that possess redox behavior include phenothiazine (PTZ),[26,27] nitroxide radicals,[28–30] π-conjugated sulfonamides,[31,32] carbonyl polymers,[33,34] etc. Among these redox polymers, organic radical polymers can be divided into two categories: *n*-type and *p*-type. Radical polymers belonging to the former class become polyanionic upon reduction and typically present potentials that are less than 3 V vs. Li^+/Li. Conversely, *p*-type radical polymers become polycationic upon oxidation, with typical potentials measuring between 3 and 4 V vs. Li^+/Li. Well-known examples of *p*-type radical polymers include those that contain 2,2,6,6-tetramethylpiperidin-1-oxyl (TEMPO) moieties, e.g., poly(TEMPO–methacrylate) (PTMA).[29] Depending on the presence of different electron-donating/withdrawing groups, TEMPO-functionalized polymers offer redox potentials between 3.5–3.6 V vs. Li/Li, robust

This article is protected by copyright. All rights reserved.

1864564x, ja, Downloaded from https://chemistry-europe.onlinelibrary.wiley.com/doi/10.1002/cssc.202500092 by A*Star Research Entities, Wiley Online Library on [19/03/2025]. See the Terms and Conditions (https://onlinelibrary.wiley.com/terms-and-conditions) on Wiley Online Library for rules of use; OA articles are governed by the applicable Creative Commons License

Accepted Manuscript

1864564x, ja, Downloaded from https://chemistry-europe.onlinelibrary.wiley.com/doi/10.1002/cssc.202500092 by A*Star Research Entities, Wiley Online Library on [19/03/2025]. See the Terms and Conditions (https://onlinelibrary.wiley.com/terms-and-conditions) on Wiley Online Library for rules of use; OA articles are governed by the applicable Creative Commons License

Accepted Manuscript

chemical stability due to resonance and steric stabilization of the radical center,[29,35,36] and stable charge/discharge up to 10 C.[37-39] Apart from TEMPO, another well-studied organic moiety that has been utilized in *p*-type polymers is PTZ. As a chemical motif for energy storage, PTZ is particularly versatile as it features a stable and reversible oxidation, a high voltage vs Li^+/Li, and high specific capacity (3.5 V vs Li/Li+ and 125.7 mAh g^{-1} per electron for *N*-methylphenothiazine).[41–46] Additionally, PTZ can undergo two consecutive single-electron oxidations from its neutral form to a radical cation and subsequently to a di-cations. These oxidative processes occur at high potentials of 3.5 V[47,48] and 4.2 V vs Li^+/Li. All factors considered, PTZ and TEMPO are regarded as promising chemical moieties for making positive electrode materials.

In this work, commodity PS from styrofoam food boxes was chemically transformed into redox-active organic polymers via a two-step functionalization sequence, without the need to pre-purify or pre-treat the styrofoam. We focused on functionalized styrenic polymers containing pendent TEMPO and PTZ moieties. Herein, we describe an expeditious two-step process for the synthesis of redox-active polymers from unpurified PS derived from commodity styrofoam food boxes. In this process, a portion of the pendent phenyl rings of PS was first chloromethylated and then further functionalized in a second step via nucleophilic substitution of the chlorides by redox-active PTZ- or TEMPO-containing moieties. The electrochemical properties of the resulting functional polymers were subsequently evaluated through cyclic voltammetry studies. Overall, the postpolymerization chemical functionalization sequence is facile and effectively transforms consumer-grade styrofoam food containers into redox-active polymers that are used as electrode materials for organic batteries.

MATERIALS AND METHODS

Phenothiazine and phenylhydrazine were purchased from TCI. All other chemicals were purchased from Sigma and used as received. Chloromethyl methyl ether (MOMCl) in

This article is protected by copyright. All rights reserved.

1864564x, ja, Downloaded from https://chemistry-europe.onlinelibrary.wiley.com/doi/10.1002/cssc.202500092 by A*Star Research Entities, Wiley Online Library on [19/03/2025]. See the Terms and Conditions (https://onlinelibrary.wiley.com/terms-and-conditions) on Wiley Online Library for rules of use; OA articles are governed by the applicable Creative Commons License

Accepted Manuscript

methyl acetate (MeOAc) was prepared according to the literature.[49] The PS starting material was taken from styrofoam food containers (product code: TA GE-203; GPC: M_n = 73.4 kDa; M_w = 194.7 kDa; $Đ$ = 2.65) from our research institute's cafeteria and this styrofoam was used directly without prior cleaning or pre-processing. Deuterated solvents for nuclear magnetic resonance (NMR) characterization were purchased from Cambridge Isotope Laboratories, Inc. Conductive carbon black C65 (MSE), Ketjen black (MSE), poly(vinylidene fluoride) (PVDF) (Merck), anhydrous *N*-methyl-2-pyrrolidone (NMP) (Merck), 1 M $LiPF_6$ in ethylene carbonate/diethyl carbonate (EC/DMC) (1:1 v/v) (Solvionic) and lithium metal foil (Gelon energy, 100 μm thickness) were used as received. LiFSI battery grade (Solvionic) was stored in an argon-filled glovebox as received and dissolved in EC/DMC (1:1 v/v) to prepare the electrolyte solution. Whatman glass fiber separators were used prior to vacuum drying at 110°C for 24 h. CR2032-coin cells were used to perform the electrochemical test.

Characterizations. NMR spectra were recorded on a 400 MHz Bruker Ultrashield Avance 400SB Spectrometer equipped with a BPO probe and variable temperature capabilities, operating at a Larmor frequency of 400.23 MHz for ^1H and 100.65 MHz for ^{13}C using deuterated methylene chloride (CD_2Cl_2) as solvent at 21 °C. For TEMPO-containing polymers, reduction with phenylhydrazine (1 drop) was first carried out before NMR acquisition so as to partially mitigate paramagnetic broadening due to the nitroxide radicals.[50,51] Gel permeation chromatography (GPC) was carried out using a Viscotek TDAmax comprised of three components: (i) GPCmax integrated solvent and sample delivery module, (ii) TDA 302 Triple Detector Array, and (iii) the OmniSEC software. The TDA 302 detector incorporates refractive index (RI) and light scattering detectors and a viscometer. Only the RI detector was used in this work. Two columns: 2 x PLgel 10 μm Mixed-B (500 to 10,000,000 Da) and 1 guard column (10 μm) were applied in sequence for separation. Tetrahydrofuran (THF) was used as the eluent

This article is protected by copyright. All rights reserved.

1864564x, ja, Downloaded from https://chemistry-europe.onlinelibrary.wiley.com/doi/10.1002/cssc.202500092 by A*Star Research Entities, Wiley Online Library on [19/03/2025]. See the Terms and Conditions (https://onlinelibrary.wiley.com/terms-and-conditions) on Wiley Online Library for rules of use; OA articles are governed by the applicable Creative Commons License

Accepted Manuscript

at a rate of 1.0 mL/min with the column and detector temperatures were set to 40 °C. The apparent polymer molecular weight and dispersity ($Đ = M_w/M_n$) were determined using conventional linear calibration based on PS standards with a calibration range of 0.580 to 3,000 kDa.

Synthesis of 30% chloromethylated PS (CMPS-30). A two-neck 100 mL round-bottom flask was fitted with a reflux condenser and a glass stopper, after which it was charged with styrofoam (2.00 g, 19.2 mmol), $ZnCl_2$ (1.60 g, 11.7 mmol), MOMCl (29.8 g, 173 mmol) in MeOAc, and CH_2Cl_2 (40 mL). The reaction mixture was then placed in an oil bath heated to 55 °C (internal temperature: 47°C) and stirred for 1 h to afford PS with a low degree of chloromethylation, i.e., 30 ± 3% of Ph rings functionalized. At the end of the reaction, the mixture was precipitated into MeOH. The precipitate was then washed with EtOH, sonicated for 5 min, and centrifuged at 7830 rpm for 5 min before the solid polymer was isolated. This purification procedure was repeated twice more, after which the isolated polymer was allowed to dry in a vacuum oven set to 40 °C. ^{1}H NMR (400 MHz, CD_2Cl_2): δ 6.20–7.40 (br, 14.3H), 4.52 (br, 2H), 1.00–2.00 (br, 3H). ^{13}C NMR (100 MHz, CD_2Cl_2): δ 145.71, 135.29, 128.42, 126.12, 46.80, 40.80. GPC (THF as eluent): M_n = 94 kDa; M_w = 363 kDa; $Đ$ = 3.87. CAUTION: As MOMCl is carcinogenic, we suggest minimizing exposure by limiting handling of the solution (in MeOAc) after it has been synthesized via the referenced procedure.[49]

Synthesis of 50% chloromethylated PS (CMPS-50). The procedure was carried out in an identical manner as with **CMPS-30** above, with the only difference being the reaction time. Here, the reaction mixture was heated for 2.5 h (instead of 1 h) to obtain PS with a medium degree of chloromethylation, i.e., 50 ± 2% of Ph rings functionalized. ^{1}H NMR (400 MHz, CD_2Cl_2): δ 6.20–7.40 (br, 4H), 4.53 (br, 1H), 1.10–2.00 (br, 3H). ^{13}C NMR (100 MHz,

This article is protected by copyright. All rights reserved.

1864564x, ja, Downloaded from https://chemistry-europe.onlinelibrary.wiley.com/doi/10.1002/cssc.202500092 by A*Star Research Entities, Wiley Online Library on [19/03/2025]. See the Terms and Conditions (https://onlinelibrary.wiley.com/terms-and-conditions) on Wiley Online Library for rules of use; OA articles are governed by the applicable Creative Commons License

Accepted Manuscript

CD_2Cl_2): δ 145.47, 134.95, 128.29, 127.86, 46.39, 40.36. GPC (THF as eluent): M_n = 83 kDa; M_w = 514 kDa; $Đ$ = 6.2.

General procedure for the synthesis of PTZ-functionalized PS. A 50 mL round-bottom flask under nitrogen was charged with NaH (0.140 g, 5.86 mmol) and DMF (30 mL) and cooled in an ice-water bath. Phenothiazine (1.17 g, 5.86 mmol) was added to the suspension and the mixture was stirred for further 15 min to deprotonate the amine. Next, the mixture was added to a two-neck 100 mL round-bottom flask containing 33% or 50% chloromethylated PS (1.00 g; which corresponds to 2.75 mmol or 3.89 mmol of CH_2Cl groups, respectively) in 30 mL of DMF. The reaction mixture was stirred overnight at 60 °C. In the case of 33% functionalized PS, at the end of the reaction the mixture was added dropwise into MeOH, and the precipitated polymer was isolated by centrifugation. The isolated polymer was dried overnight at 40 °C in a vacuum oven. **PS-PTZ-33** from 33% chloromethylated PS: Yield: 0.80 g, 55 %. ^{1}H NMR (400 MHz, CD_2Cl_2): δ 6.00–7.60 (br, 24H), 4.90 (br, 2H), 0.90–2.50 (br, 12H). GPC (THF as eluent): M_n = 83 kDa; M_w = 514 kDa; $Đ$ = 6.2. In the case of 50% functionalized PS, precipitation of the 43% PTZ-substituted polymer product occurred after overnight reaction and this was isolated and dried in a similar fashion. **PS-PTZ-43** from 50% chloromethylated PS: Yield: 1.3 g, 80 %. ^{1}H NMR (400 MHz, CD_2Cl_2): δ 5.80 – 7.40 (br, 18.5H), 4.87 (br, 2H), 4.42 (br, 0.32 H), 0.92 – 2.10 (br, 8.6H).

General procedure for the synthesis of TEMPO-functionalized PS. A stirred suspension of NaH (0.72 g, 30 mmol) in DMF (90 mL) contained in a 500-mL two-neck round-bottom flask under nitrogen atmosphere was first cooled in an ice-water bath. Next, a solution of 4-hydroxy-TEMPO (4.20 g, 24.4 mmol) in DMF (60 mL) was added dropwise to the mixture. This reaction mixture was stirred for a further 30 min to deprotonate the alcohol, after which 27% or 52% chloromethylated PS (1.80 g, corresponding to 4.15 mmol or 7.24 mmol of

This article is protected by copyright. All rights reserved.

1864564x, ja, Downloaded from https://chemistry-europe.onlinelibrary.wiley.com/doi/10.1002/cssc.202500092 by A*Star Research Entities, Wiley Online Library on [19/03/2025]. See the Terms and Conditions (https://onlinelibrary.wiley.com/terms-and-conditions) on Wiley Online Library for rules of use; OA articles are governed by the applicable Creative Commons License

Accepted Manuscript

CH_2Cl groups, respectively) in 60 mL of DMF was added to the reaction mixture. The ice bath was removed, and the stirred reaction mixture was allowed to warm up to room temperature before being heated at 65 °C for the next 24 h. Upon reaction completion, the mixture was precipitated into Et_2O, and the supernatant liquid was decanted. The precipitated polymer was washed in ultrapure water once, centrifuged, and decanted again. The residue was then subjected to two rounds of washing with Et_2O, centrifugation, and decanting to afford a purified solid. This isolated solid was dried overnight in a vacuum oven at 40 °C. **PS-TEMPO-27** from 27% chloromethylated PS: Yield: 1.55 g, 65 %. ^{1}H NMR (400 MHz, CD_2Cl_2 + 1 drop of phenylhydrazine): δ 6.60–7.60 (br), 4.86 (br), 3.64 (br), 1.92 (br), 1.00–1.50 (br). **PS-TEMPO-52** from 52% chloromethylated PS: Yield: 0.74 g, 27 %. ^{1}H NMR (400 MHz, CD_2Cl_2 + 1 drop of phenylhydrazine): δ 6.50–7.70 (br), 4.82 (br), 3.62 (br), 2.06 (br), 1.00–1.60 (br). N.B.: phenylhydrazine was added to the NMR sample to mitigate the pronounced paramagnetic broadening effect of the nitroxide radicals.

Electrochemical characterization.

Thorough electrochemical investigations were conducted on the redox-active materials, by testing their redox activity in a three-electrode liquid cell: a glassy carbon electrode coated with **PS-PTZ-33**:C65:PVDF slurry (weight ratio 20:70:10) was used as working electrode after being dried under vacuum at 70 °C overnight; a Pt wire and a Ag wire were used as counter electrode and reference electrode, respectively. A 0.1 M solution of $LiClO_4$ in acetonitrile was used as electrolyte under nitrogen flux. The redox-active material was mixed with conductive carbon (C65) in a ball-mill (FRITSCH, pulverisette 7) for 5 min at 500 rpm. A homogeneous slurry of the powders and PVDF solution in NMP (5% wt.) was obtained by mixing the PVDF solution and the powder mixture in a SpeedMixer (FlackTek DAC 330-100 SE) at 1500 rpm for a total of 10 min. The same process was used for the investigation of **PS-PTZ-43** in a three-

This article is protected by copyright. All rights reserved.

1864564x, ja, Downloaded from https://chemistry-europe.onlinelibrary.wiley.com/doi/10.1002/cssc.202500092 by A*Star Research Entities, Wiley Online Library on [19/03/2025]. See the Terms and Conditions (https://onlinelibrary.wiley.com/terms-and-conditions) on Wiley Online Library for rules of use; OA articles are governed by the applicable Creative Commons License

Accepted Manuscript

electrode liquid cell. The same slurry preparation protocol was used for all four redox-active polymers (i.e., **PS-PTZ-33**, **PS-PTZ-43**, **PS-TEMPO-27**, and **PS-PTZ-52**) to obtain coated glassy carbon electrodes and aluminum-coated electrodes used in the coin cells (CR2032). The latter were prepared by casting the slurry onto an Al-carbon coated foil using an automatic doctor blade with a 100 μm-thick wet slurry layer. The electrode foils were dried overnight at 60 °C and the prepared 12 mm diameter disks where further dried overnight at 80 °C under vacuum prior to being transferred into an argon-filled glovebox (O_2 and H_2O levels < 1 ppm). The prepared redox electrodes were used in combination with Li metal to assemble lab-scale half-cells. Lithium metal disks were used as the anode and reference electrode. **PS-PTZ-33**, **PS-PTZ-43, PS-T-27** and **PS-T-52** were also tested using conductive Ketjen black (KJB) in place of C65 with the same protocol. Cyclic voltammograms were performed between 3 and 4 V vs Li^+/Li at different scan rates (i.e., 1, 10, 20, 30, 40, and 50 mV s^{-2}) using a VMP3 Potentiostat (BioLogic). Galvanostatic cycling were performed in the voltage range between 3–3.8 V at laboratory room temperature using battery cycler equipment (Neware) at different C-rates (i.e., C/3 for 5 cycles, 1C for 5 cycles, 1.5 C for 5 cycles, and C/3 for 100 cycles for C65-based electrode and C/10 for 5 cycles, C/5 for 5 cycles, C/2 for 5 cycles, and 1C until the 100^{th} cycle for KJB-based electrodes).

RESULTS AND DISCUSSION

Functionalization of commodity styrofoam

Commodity PS derived from styrofoam food containers from our research institute's cafeteria was used as the starting material in our two-step synthesis of redox-active polymers. Pre-treatment or cleansing of the styrofoam was not required. Utilizing commodity PS as an inexpensive and readily available raw material removes the need for monomer synthesis as well as any subsequent polymerization. Instead, it allows us to leverage the large-scale, low-cost industrial production of a ubiquitous aromatic polymer that can serve as a precursor to

This article is protected by copyright. All rights reserved.

complex and tailorable functional materials for myriad applications. Furthermore, styrofoam or expanded PS is also typically non-recyclable due to the unfavorable economics associated with its low density and high bulk.[2] Thus, devising new ways to upcycle the polymer could potentially reduce the volume of PS waste that goes into landfills and incinerators. Chemically, commodity PS presents a ready-made macromolecular structure with a wealth of aromatic rings with wide chemical reactivity. In essence, PS may be regarded as a 'blank slate' polymer whose materials properties can be tailored at will for different applications via the postpolymerization introduction of specific functionality. Indeed, we have previously demonstrated the chemical upcycling of commodity PS to produce broad-spectrum antimicrobial fabrics.[9] In that study, quantitative chloromethylation (i.e., one CH_2Cl group for every repeat unit) was employed successfully under judiciously optimized conditions. In the present study however, exhaustively chloromethylated PS proved infeasible as a precursor to redox-active polymers due to subsequent solubility problems that will be discussed below. Instead, it was necessary to fine-tune the degree of pendent functionalization to circumvent these issues. Gratifyingly, we found that the use of short reaction times between 1 to 3 h enabled the reliable preparation of low-to-moderate (~30–50%) degrees of chloromethylation to within 2–3%. Subsequent optimization showed that 30 ± 3% chloromethylated PS (**CMPS-30**) and 50 ± 3% chloromethylated PS (**CMPS-50**) were afforded when reaction times of 1 h and 2.5 h were used, respectively. As precursors, these functionalized styrenic polymers were found to be readily converted into PTZ- and TEMPO-containing redox polymers through simple S_N2 chemistry in the next step.

This article is protected by copyright. All rights reserved.

1864564x, ja, Downloaded from https://chemistry-europe.onlinelibrary.wiley.com/doi/10.1002/cssc.202500092 by A*Star Research Entities, Wiley Online Library on [19/03/2025]. See the Terms and Conditions (https://onlinelibrary.wiley.com/terms-and-conditions) on Wiley Online Library for rules of use; OA articles are governed by the applicable Creative Commons License

Accepted Manuscript

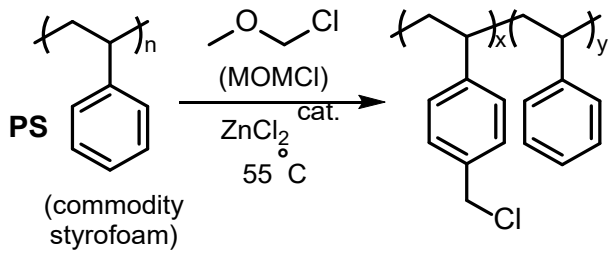

Reaction time (h)	x (%)	y (%)	Polymer
1	~30	~70	CMPS-30
2.5	~50	~50	CMPS-50
24	~100	~0	CMPS

Figure 1. Synthesis of chloromethylated PS with different degrees of functionalization depending on reaction time used.

Introducing redox-active moieties onto the polymer

Following the synthesis of ~30% and ~50% CMPS, the second (and final) step involved introducing redox-active moieties into the polymer via nucleophilic displacement of the chlorides. To achieve this, phenothiazine and 4-hydroxy-TEMPO were used as the reagents, since both molecular motifs are capable of *p*-type single-electron redox processes. The chemical functionalization process was conceptually straightforward but practically challenging. In brief, the reagents were deprotonated with NaH and then reacted with CMPS to install the redox-active groups. However, it was during this phase of the chemical conversion sequence that the importance of the degree of PS halomethylation quickly became apparent. In our preliminary studies, 100% chloromethylated PS was initially employed. Unfortunately, it was observed that a solubility limit was reached after a certain percentage of chlorides were substituted by TEMPO or PTZ. This resulted in polymer precipitation and consequently the premature cessation of the reaction. Through screening and optimization studies, we found that the solubility threshold was crossed whenever the PS chain became ~40–50% randomly functionalized with pendent TEMPO or PTZ groups. Ultimately, starting from **CMPS-30** and **CMPS-50**, we were able to prepare four redox-active polymers for electrochemical studies: **PS-TEMPO-27**, **PS-TEMPO-52**, **PS-PTZ-33**, and **PS-PTZ-43**. The first two random polymers featured a PS chain with 27% and 52% of its repeat units bearing pendent TEMPO

This article is protected by copyright. All rights reserved.

1864564x, ja, Downloaded from https://chemistry-europe.onlinelibrary.wiley.com/doi/10.1002/cssc.202500092 by A*Star Research Entities, Wiley Online Library on [19/03/2025]. See the Terms and Conditions (https://onlinelibrary.wiley.com/terms-and-conditions) on Wiley Online Library for rules of use; OA articles are governed by the applicable Creative Commons License

Accepted Manuscript

moieties, respectively, while the third and fourth contained chains that were 33% and 43% randomly functionalized with pendent PTZ groups.

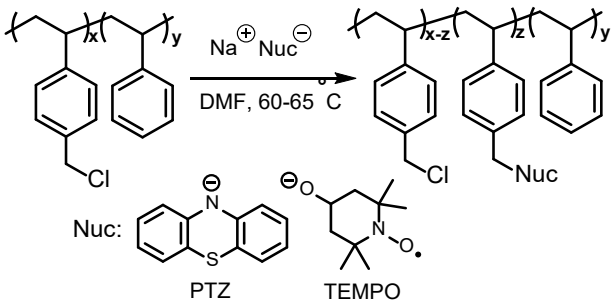

Nuc	x (%)	y (%)	z (%)	Polymer
TEMPO	27	73	27	PS-TEMPO-27
TEMPO	52	48	52	PS-TEMPO-52
PTZ	33	67	33	PS-PTZ-33
PTZ	50	50	43	PS-PTZ-43

Figure 2. Synthesis of redox-active polymers from partially chloromethylated PS.

Electrochemical characterization of the redox-active PS

The solubilities of our redox-active polymers in electrolyte were tested by immersing them in liquid electrolyte solution ($LiPF_6$ in EC:DEC) within a glovebox to avoid moisture contamination. The mixtures were then stirred overnight at 25 ºC. As illustrated in Figure S10, the liquid phase did not present color changes, indicating the insoluble nature of the polymers. Moreover, even when stirred overnight, the PS-TEMPOs did not deagglomerate, whereas the PS-PTZs became suspensions within the electrolyte but did not dissolve. The marked insolubility of these PS-derived polymers promised good stability as electrode materials. Preliminary assessment of the redox activities of the PTZ-based polymers was performed in a liquid three-electrode cell by cyclic voltammetry at 1 mV s^{-1} as reported in Figure S11 (Supporting information). Both **PS-PTZ-33** and **PS-PTZ-43** demonstrated highly reversible redox activity with the formation of radical cations, neutralized by the ClO_4^- anions, with a half-wave potential $E_{1/2}$ of 0.7 V vs Ag wire and a separation between anodic and cathodic peaks (ΔE) of ~10 mV for both systems, indicating a fully reversible redox process. Cyclic voltammetry at 1 mV s^{-1} (Figure 3) and at increasing scan rates (i.e., 10, 20, 30, 40, and 50 mV s^{-1}) (Figure 4) were also carried out in a Li-metal half-cell using 1 M $LiPF_6$ in EC:DEC (1:1

This article is protected by copyright. All rights reserved.

1864564x, ja, Downloaded from https://chemistry-europe.onlinelibrary.wiley.com/doi/10.1002/cssc.202500092 by A*Star Research Entities, Wiley Online Library on [19/03/2025]. See the Terms and Conditions (https://onlinelibrary.wiley.com/terms-and-conditions) on Wiley Online Library for rules of use; OA articles are governed by the applicable Creative Commons License

Accepted Manuscript

1864564x, ja, Downloaded from https://chemistry-europe.onlinelibrary.wiley.com/doi/10.1002/cssc.202500092 by A*Star Research Entities, Wiley Online Library on [19/03/2025]. See the Terms and Conditions (https://onlinelibrary.wiley.com/terms-and-conditions) on Wiley Online Library for rules of use; OA articles are governed by the applicable Creative Commons License

Accepted Manuscript

vol%) electrolyte. As displayed in Figure 3, the oxidation of **PS-PTZ-33** and **PS-PTZ-43** occurred at the first cycle at 3.71 and 3.74 V, respectively. However, after six cycles at 1 mV s^{-1}, the oxidation peak of **PS-PTZ-33** shifted to 3.73 V, while in the peak in the **PS-PTZ-43** system shifted to 3.71 V. On the other side, the reduction of **PS-PTZ-33** occurred stably at 3.54 V while the **PS-PTZ-43** reduction peak shifted from 3.58 to 3.54 V. The peak shift observed for the **PS-PTZ-43**, may suggest modifications at the electrode interface that could be related to the lingering presence of unconverted benzylic chloride moieties in this specific polymer. Nevertheless, both electrodes showed electron transfer-controlled behavior with ΔE of 20 mV for **PS-PTZ-33** and 15 mV for **PS-PTZ-43**. In contrast, when the scan rate was increased, the timescale of the experiment inevitably competes with the timescale of the redox reactions, as shown in Figure 4, where the ΔE increase with the scan rates, suggesting a mass diffusion-controlled process.

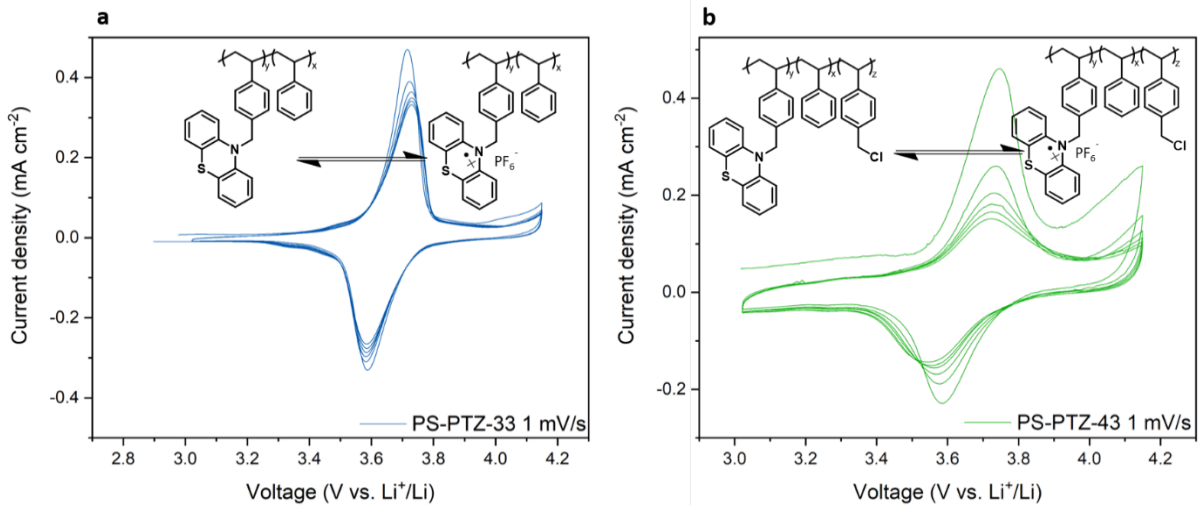

Figure 3. Cyclic voltammetry at 1 mV s^{-1} of Li-metal half cells with (a) **PS-PTZ-33** and (b) **PS-PTZ-43** cathodes.

This article is protected by copyright. All rights reserved.

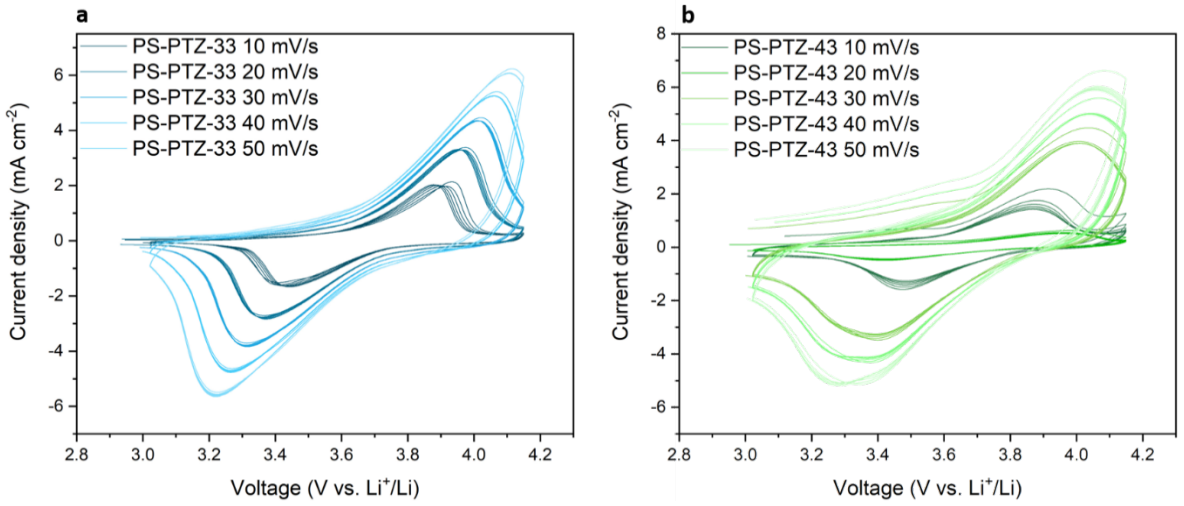

Figure 4. Cyclic voltammetry at increasing scan rate of Li-metal half cells with (a) **PS-PTZ-33** and (b) **PS-PTZ-43** cathodes.

Similar results were also obtained for the TEMPO-functionalized redox polymers **PS-TEMPO-27** and **PS-TEMPO-52**, which were characterized by CV at 10 mV s^{-1}. The organic electrodes prepared using C65 were tested in Li metal half-cell configurations with 1 M $LiPF_6$ in EC:DEC. Results for both TEMPO systems (Figure 5) indicated excellent reversibility with a half-wave potential $E_{1/2}$ of 3.58 V. Negligible peak shifting as a function of the scan rate was also observed (Figure 6), suggesting a diffusion-controlled process.

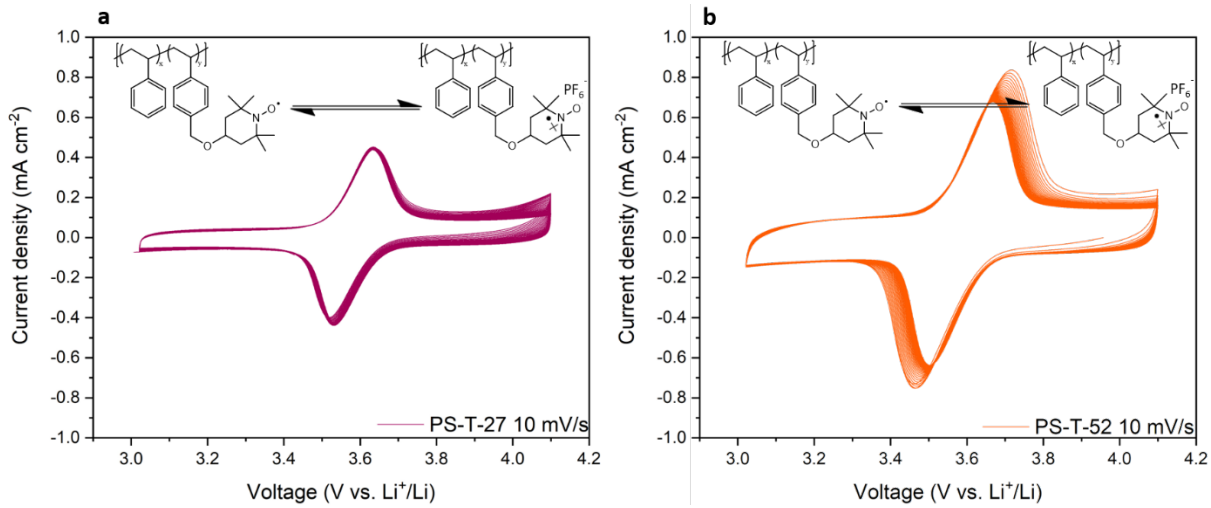

Figure 5. Cyclic voltammetry at 10 mV s^{-1} of Li-metal half-cells with (a) **PS-TEMPO-27** and (b) **PS-TEMPO-52** cathodes.

This article is protected by copyright. All rights reserved.

1864564x, ja, Downloaded from https://chemistry-europe.onlinelibrary.wiley.com/doi/10.1002/cssc.202500092 by A*Star Research Entities, Wiley Online Library on [19/03/2025]. See the Terms and Conditions (https://onlinelibrary.wiley.com/terms-and-conditions) on Wiley Online Library for rules of use; OA articles are governed by the applicable Creative Commons License

Accepted Manuscript

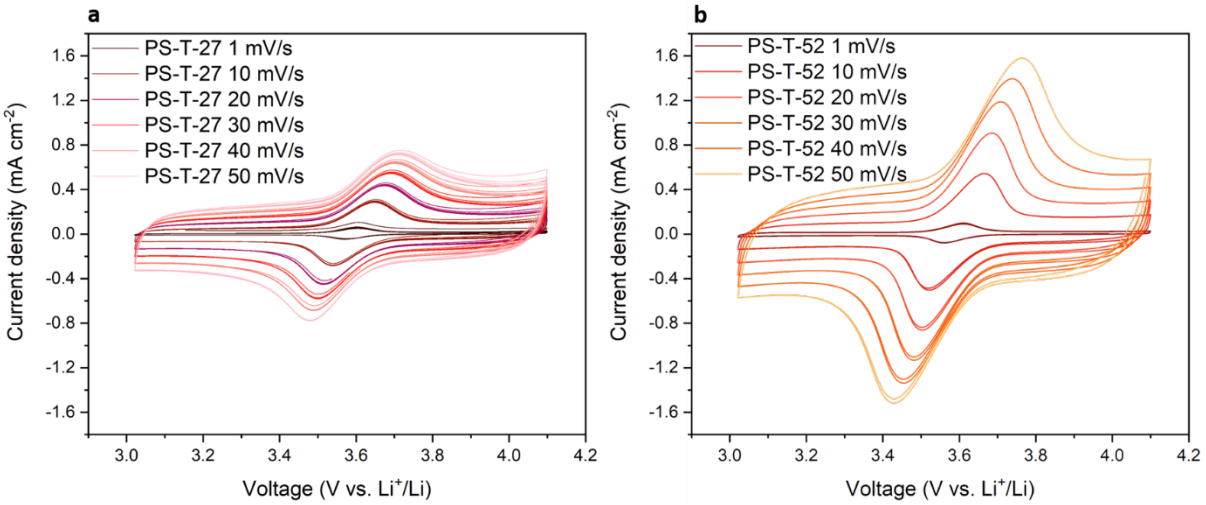

Figure 6. Cyclic voltammetry at increasing scan rates of Li-metal half-cells with (a) **PS-TEMPO-27** and (b) **PS-TEMPO-52** cathodes.

After the redox activities of both sets of polymers were assessed by cyclic voltammetry, the electrochemical performance of the PTZ-based ones were investigated by means of galvanostatic cycling (GC) at different C-rates in Li-metal half-cells at ambient temperature. We recognized that the PS-PTZs could be used as organic cathode materials since they performed at redox potentials higher than 3.5 V. Thus, the GCs were conducted between 3 and 3.8 V, at C/3, 1C, 1.5C for five cycles at each C-rate and then at C/3 until 100 cycles were completed. The C-rate currents were calculated based on theoretical capacities of 96 and 67 mAh g^{-1} for **PS-PTZ-33** and **PS-PTZ-43**, respectively. Calculation of these theoretical specific capacities was carried out based on the percentage of repeat units bearing redox-active pendant moieties. As shown in Figure S12 of the Supporting Information, both the PTZ-based polymers in conjunction with conductive carbon C65 and 1 M $LiPF_6$ in EC:DEC (1:1 vol%) as liquid electrolyte performed similarly, delivering an average specific discharge capacity output of 30 mAh g^{-1} and 20 mAh g^{-1} for **PS-PTZ-33** and **PS-PTZ-43**, respectively. Given its low specific surface area, commercial carbon C65 may not guarantee homogeneous distribution of the active materials, thus partially limiting electron conduction and ion diffusion, which

This article is protected by copyright. All rights reserved.

1864564x, ja, Downloaded from https://chemistry-europe.onlinelibrary.wiley.com/doi/10.1002/cssc.202500092 by A*Star Research Entities, Wiley Online Library on [19/03/2025]. See the Terms and Conditions (https://onlinelibrary.wiley.com/terms-and-conditions) on Wiley Online Library for rules of use; OA articles are governed by the applicable Creative Commons License

Accepted Manuscript

consequently reduces cell performance.[52] For this reason, conductive carbon KJB, characterized by higher specific surface area and mesoporous structure, was implemented in place of C65. The **PS-PTZ-33** and **PS-PTZ-43** systems with KJB (**PS-PTZ-33 KJB** and **PS-PTZ-43 KJB**) were cycled at different C-rates (i.e., C/10 for 5 cycles, C/5 for 5 cycles, C/2 for 5 cycles, 1C until 100 cycles are completed, in Figure 7). The KJB-systems with 1 M $LiPF_6$ in EC:DEC (1:1, vol %) as electrolyte showed performances in line with other phenothiazine-based cathodes (see **Table S1**).[53,54] In particular, **PS-PTZ-33 KJB** showed a specific capacity of 45 mAh g^{-1} at 1C, while **PS-PTZ-43 KJB** gave an output of 60 mAh g^{-1}, corresponding to almost 47% and 90% of the theoretical capacities, respectively. At low C-rates, both redox polymers displayed different oxidation and reduction behavior, with the oxidation process characterized by larger plateaus along with higher capacity with respect to the reduction. This behavior can be attributed to less favorable kinetics associated with ion insertion, as shown by the potential profiles in Figure S13 in the Supporting Information. Indeed, possible equilibration and Solid Electrolyte Interface (SEI) formation process are excluded. On the other hand, the discharge capacity was practically constant per each C-rate, and at 1C C-rate, coulombic efficiencies (CE) of 94% for **PS-PTZ-33 KJB** and 97% for **PS-PTZ-43 KJB** were attained. Indeed, these CE values were much more stable and higher compared to samples with C65 (i.e., 80% and 95% for **PS-PTZ-33** and **PS-PTZ-43**, respectively - Figure S12) due to increased homogeneous electronic conduction provided by the KJB. Moreover, discharge capacity retention values of 95% at 1C C-rate current were observed for both the **PS-PTZ-33** and **PS-PTZ-43** samples.

This article is protected by copyright. All rights reserved.

1864564x, ja, Downloaded from https://chemistry-europe.onlinelibrary.wiley.com/doi/10.1002/cssc.202500092 by A*Star Research Entities, Wiley Online Library on [19/03/2025]. See the Terms and Conditions (https://onlinelibrary.wiley.com/terms-and-conditions) on Wiley Online Library for rules of use; OA articles are governed by the applicable Creative Commons License

Accepted Manuscript

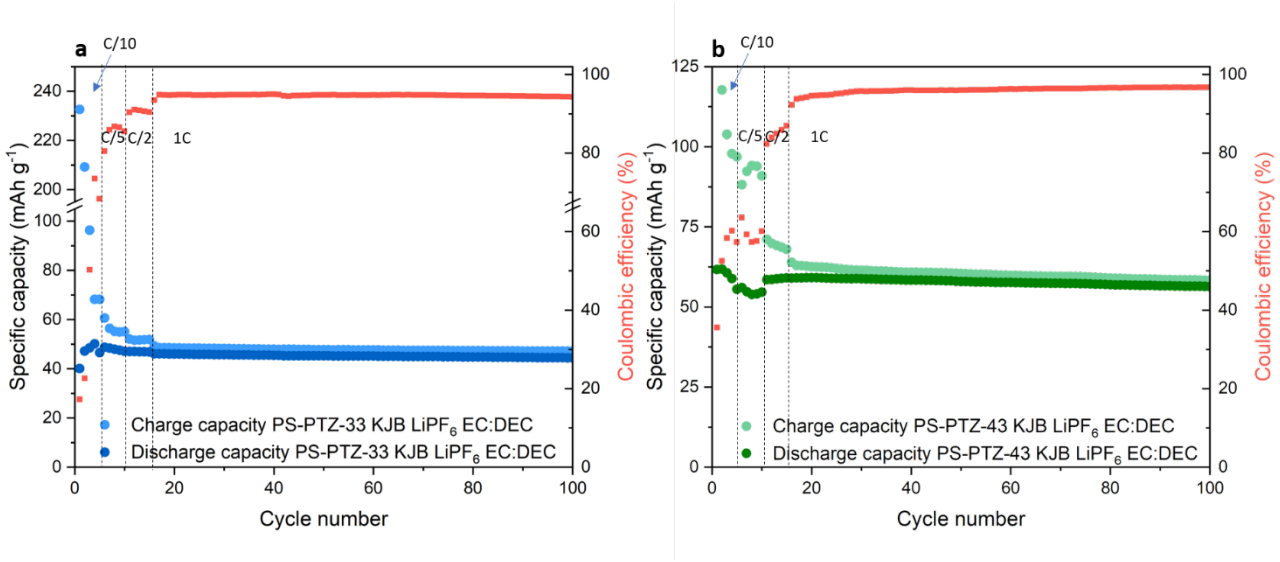

Figure 7. Galvanostatic rate performance of lithium half-cells with 1M $LiPF_6$ in EC:DEC electrolyte and redox polymers (a) **PS-PTZ-33 KJB** or (b) **PS-PTZ-43 KJB**.

Replacing the $LiPF_6$-based electrolyte with 1 M LiFSI EC:DMC (1:1 vol %) facilitated the further increase of CE values to 98% for both samples, likely due to improved ionic conductivity and better SEI forming ability of the FSI-based salt relative to the PF_6-based one, which favors the formation of a more stable and conductive electrolyte/electrode interface.[55] In addition, both **PS-PTZ-33 KJB** and **PS-PTZ-43 KJB** cycled with 1 M LiFSI in EC:DMC (Figure 8) displayed similar specific capacity values around 50 mAh g^{-1} at 1C C-rate current, retaining 85% and 80% of the first cycle discharge capacity, respectively. It is worth noting that **PS-PTZ-33 KJB** in combination with both LiFSI- and $LiPF_6$-based electrolytes delivered similar specific capacity values, whereas **PS-PTZ-43 KJB** with LiFSI in EC:DMC electrolyte exhibited slightly lower values in comparison with the counterpart using $LiPF_6$ in EC:DMC, suggesting that the anion-polycation interaction during the oxidation/reduction process and the resulting specific capacity output are strongly correlated to the chemical nature of the coordinating anions of the electrolyte.[56,57]

This article is protected by copyright. All rights reserved.

1864564x, ja, Downloaded from https://chemistry-europe.onlinelibrary.wiley.com/doi/10.1002/cssc.202500092 by A*Star Research Entities, Wiley Online Library on [19/03/2025]. See the Terms and Conditions (https://onlinelibrary.wiley.com/terms-and-conditions) on Wiley Online Library for rules of use; OA articles are governed by the applicable Creative Commons License

Accepted Manuscript

10.1002/cssc.202500092

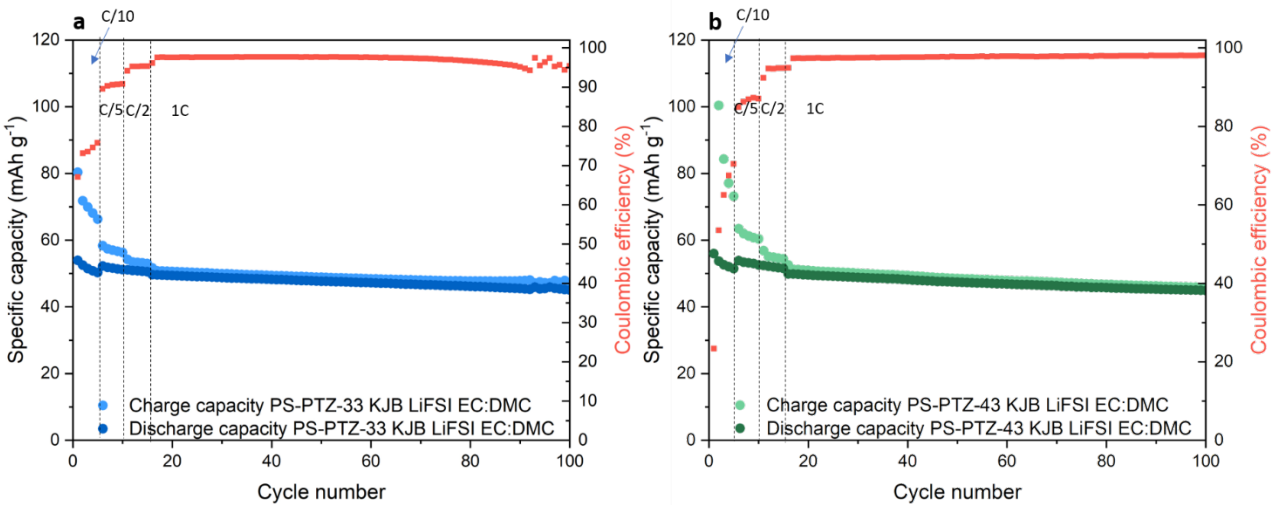

Figure 8. Galvanostatic rate performance of lithium half-cells using a 1M LiFSI in EC:DMC electrolyte and redox polymer (a) **PS-PTZ-33 KJB** or (b) **PS-PTZ-43 KJB**.

The optimal electrochemical configuration and protocol were applied to the TEMPO-based redox polymers as well. **PS-TEMPO-27** and **PS-TEMPO-52** organic electrodes were prepared with KJB using a proportion of 20:70, and half-cells in combination with $LiPF_6$ in EC:DEC electrolyte underwent the same rate performance protocol (i.e., C/10 for 5 cycles, C/5 for 5 cycles, C/2 for 5 cycles, and 1C until 100 cycles were completed). The results shown in Figure 9 depict promising performances, which could be improved with further optimization of the electrode preparation process. Indeed, **PS-TEMPO-27** showed slightly lower capacity values with respect to **PS-TEMPO-52** (i.e., 30 mAh g^{-1} vs. 40 mAh g^{-1} at 1C) as well as lower coulombic efficiency. Nevertheless, the results obtained for **PS-TEMPO-52** are on par with values currently reported in the literature, as illustrated in Table S2. The pronounced insolubility of these PS-derived redox polymers, guarantee great capacity retention at the 100th cycle at 1C, namely 96.4 % and 92.7 % for **PS-TEMPO-27** and **PS-TEMPO-52,** respectively.

This article is protected by copyright. All rights reserved.

1864564x, ja, Downloaded from https://chemistry-europe.onlinelibrary.wiley.com/doi/10.1002/cssc.202500092 by A*Star Research Entities, Wiley Online Library on [19/03/2025]. See the Terms and Conditions (https://onlinelibrary.wiley.com/terms-and-conditions) on Wiley Online Library for rules of use; OA articles are governed by the applicable Creative Commons License

Accepted Manuscript

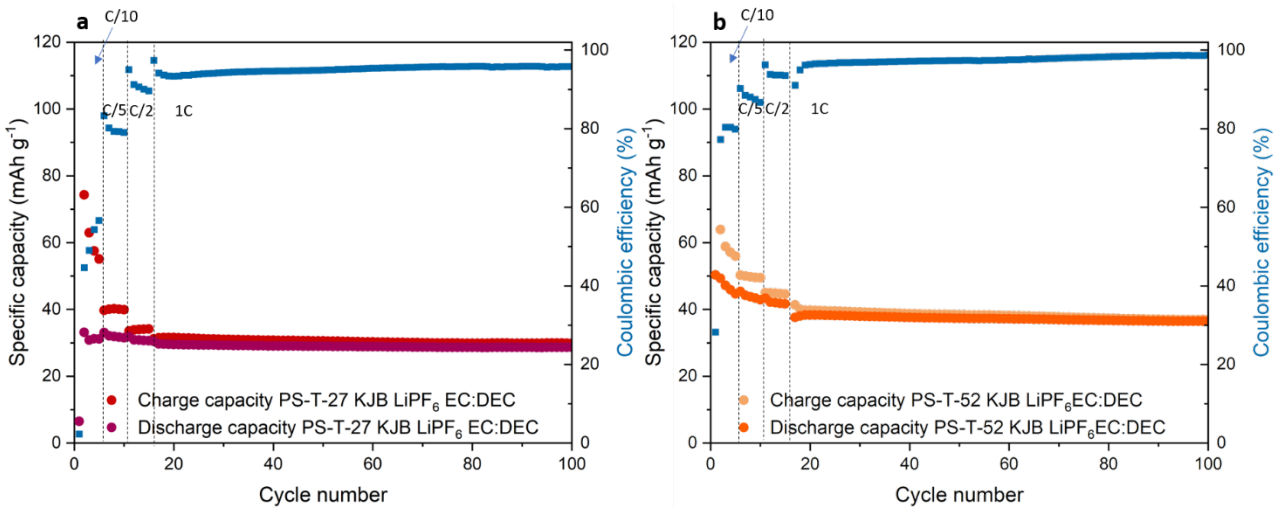

Figure 9. Galvanostatic rate performance of lithium half-cells using a 1M $LiPF_6$ in EC:DEC electrolyte and redox polymer (a) **PS-TEMPO-27 KJB** or (b) **PS-TEMPO-52 KJB**.

CONCLUSIONS

In this study, PS from commodity styrofoam food boxes were upcycled into redox-active polymers via postpolymerization functionalization, without the need for prior cleansing or pre-treatment of the starting material. This was a two-step sequence involving controlled chloromethylation of 30–50% of the PS phenyl sidechains, followed by the installation of redox-active PTZ and TEMPO moieties via nucleophilic substitution. The resulting functional polymers were studied by cyclic voltammetry and found to be viable as cathode materials. Subsequently, their electrochemical performance was investigated through galvanostatic cycling with two different types of conductive carbon, namely C65 and KJB, and two different electrolytes. This study revealed the optimal electrochemical conditions that showcased the potential of postconsumer PS as a precursor to cathode materials for Li-ion batteries. Empirically, optimal performance was realized when the redox polymers were compounded in a way that provided intimate contact with the conductive agent, and this was made possible by using mesoporous KJB instead of carbon C65. For instance, **PS-PTZ-43 KJB** in combination

This article is protected by copyright. All rights reserved.

1864564x, ja, Downloaded from https://chemistry-europe.onlinelibrary.wiley.com/doi/10.1002/cssc.202500092 by A*Star Research Entities, Wiley Online Library on [19/03/2025]. See the Terms and Conditions (https://onlinelibrary.wiley.com/terms-and-conditions) on Wiley Online Library for rules of use; OA articles are governed by the applicable Creative Commons License

Accepted Manuscript

1864564x, ja, Downloaded from https://chemistry-europe.onlinelibrary.wiley.com/doi/10.1002/cssc.202500092 by A*Star Research Entities, Wiley Online Library on [19/03/2025]. See the Terms and Conditions (https://onlinelibrary.wiley.com/terms-and-conditions) on Wiley Online Library for rules of use; OA articles are governed by the applicable Creative Commons License

Accepted Manuscript

with $LiPF_6$ in EC:DE afforded a discharge capacity of 60 mAh g^{-1} at 1C with a capacity retention of 91% for the first cycle. Meanwhile, the TEMPO-based materials **PS-TEMPO-27 KJB** and **PS-TEMPO-52 KJB** achieved capacity retentions of 96.4% and 92.7% at 1C and discharge capacity values of about 30 and 40 mAh g^{-1}, respectively. Additionally, we also found that for PS-PTZs, switching the electrolyte to LiFSI boosted CE values, likely due to the formation of a more conductive electrode/electrolyte interface. In conclusion, this work provides proof-of-concept that used commodity PS—and potentially other plastics as well—could serve as essentially cost-free precursors to functional materials for energy storage applications. Ultimately, our ability to leverage postconsumer polymers as a raw material could alleviate the burden on petroleum reserves for the synthesis of high-value specialty materials.

ASSOCIATED CONTENT

Supporting Information

The supporting information is available free of charge at https://pub.acs.org/doi/

Characterization data, ^{1}H and ^{13}C NMR spectra.

Author Contributions

The manuscript was written with the contributions of all authors. All authors have given approval to the final version of this manuscript.

Notes

The authors declare no competing financial interest.

This article is protected by copyright. All rights reserved.

1864564x, ja, Downloaded from https://chemistry-europe.onlinelibrary.wiley.com/doi/10.1002/cssc.202500092 by A*Star Research Entities, Wiley Online Library on [19/03/2025]. See the Terms and Conditions (https://onlinelibrary.wiley.com/terms-and-conditions) on Wiley Online Library for rules of use; OA articles are governed by the applicable Creative Commons License

Accepted Manuscript

ACKNOWLEDGMENTS

This research was supported by the Agency for Science, Technology and Research (A*STAR) under its Career Development Fund (Project No. C210812024). J. M. W. C. is supported by A*STAR under its 2022 SERC Central Research Fund UIBR. G.L. acknowledges funding from the European Union's Horizon 2020 Research and Innovation Programme under the Marie Skłodowska-Curie grant agreement No. 101034379. H.S. acknowledges grant TED2021-129852B-C22 funded by MCIU/AEI/10.13039/501100011033. The authors also acknowledge grant PLEC2021-007929 funded by MCIU/AEI/10.13039/501100011033 and by the European Union NextGenerationEU/PRTR and grant PID2023-153050OB-I00 funded by MCIU/AEI/10.13039/501100011033 and by ERDF/EU.

REFERENCES

[1] A. Chamas, H. Moon, J. Zheng, Y. Qiu, T. Tabassum, J. H. Jang, M. Abu-Omar, S. L. Scott, S. Suh, *ACS Sustain. Chem. Eng*. 2020, **8**, 3494–3511.

[2] A. Rahimi, J. M. García, *Nat. Chem. Rev*. 2017, **1**, 0046.

[3] S. E. Lewis, B. E. Wilhelmy Jr, F. A. Leibfarth, *Polym. Chem*. 2020, **11**, 4914–4919.

[4] S. E. Lewis, B. E. Wilhelmy Jr, F. A. Leibfarth, *Chem. Sci*. 2019, **10**, 6270–6277.

[5] B. P. Jacobs, J. N. Brantley, *Macromolecules* 2020, **53**, 9287−9293.

[6] B. Dou, Y. Xu, J. Wang, *J. Am. Chem. Soc*. 2023, **145**, 10422−10430.

[7] B. Xue, P. P. Huang, M. Z. Zhu, S. Q. Fu, J. H. Ge, X. Li, P. N. Liu, *ACS Macro Lett*. 2022, **11**, 1252−1257.

[8] J. Shin, S. M. Jensen, J. Ju, S. Lee, Z. Xue, S. K. Noh, C. Bae, *Macromolecules* 2007, **40**, 8600−8608.

[9] A. O. Biying, M. J. H. Ong, W. Zhao, N. Li, H.-K. Luo, J. M. W. Chan*, ACS Appl. Polym. Mater*. 2024, **6**, 8169−8177.

This article is protected by copyright. All rights reserved.

[10] C.-Y. Lo, K. P. Koutsoukos, M. N. Dan, Y. Wu, D. A. A. Trujillo, T. Miller, T. Shrestha, E. Mackey, D. S. Damani, U. Kanbur, R. Opila, D. C. Martin, D. Kaphan, L. V. Kayser, *JACS Au* 2024, **4**, 2596–2605.

[11] Z. S. Pour, P. S. Shinde, J. E. Bara, *ACS Appl. Polym. Mater.* 2024, **6**, 14309–14319.

[12] Z. Zhao, C. Zhang, X. Li, *J. Energy Chem*. 2022, **67**, 621–639.

[13] T. Katsumata, H. Yamamoto, Y. Kimura, K. Amezawa, R. Aso, S. Kikkawa, S. Yamazoe, T. Nakamura, *Adv. Funct. Mater*. 2023, **33**, 2307116.

[14] Y. Zhao, O. Pohl, A. I. Bhatt, G. E. Collis, P. J. Mahon, T. Rüther, A. F. Hollenkamp, *Sustainable Chem*. 2021, **2**, 167–205.

[15] M. K. Tran, M. T. F. Rodrigues, K. Kato, G. Babu, P. M. Ajayan, *Nat. Energy* 2019, **4**, 339–345.

[16] P. Poizot, J. Gaubicher, S. Renault, L. Dubois, Y. Liang, Y. Yao, *Chem. Rev*. 2020, **120**, 6490–6557.

[17] E. Fan, L. Li, Z. Wang, J. Lin, Y. Huang, Y. Yao, R. Chen, F. Wu, *Chem. Rev*. 2020, **120**, 7020–7063.

[18] C. Banza Lubaba Nkulu, L. Casas, V. Haufroid, T. De Putter, N. D. Saenen, T. Kayembe-Kitenge, P. Musa Obadia, D. Kyanika Wa Mukoma, J. M. Lunda Ilunga, T. S. Nawrot, O. L. Numbi, E. Smolders, B. Nemery, *Nat. Sustain*. 2018, **1**, 495–504.

[19] M. Li, R. Wang, T. Wu, Y. Liu, Y. Chen, W. He, S. Feng, X. Zhang, G. Dai, Y. Zhao, *ACS Appl. Energy Mater*. 2023, **6**, 6834–6841.

[20] R. M. Thakur, T. Ma, G. Shamblin, S. S. Oka, S. M. Lalwani, A. D. Easley, J. L. Lutkenhaus, *ChemSusChem* 2024, e202400788.

[21] J. Kim, Y. Kim, J. Yoo, G. Kwon, Y. Ko, K. Kang, *Nat. Rev. Mater*. 2022, **8**, 54–70.

[22] N. Goujon, N. Casado, N. Patil, R. Marcilla, D. Mecerreyes, *Prog. Polym. Sci*. 2021, **122**, 101449.

This article is protected by copyright. All rights reserved.

1864564x, ja, Downloaded from https://chemistry-europe.onlinelibrary.wiley.com/doi/10.1002/cssc.202500092 by A*Star Research Entities, Wiley Online Library on [19/03/2025]. See the Terms and Conditions (https://onlinelibrary.wiley.com/terms-and-conditions) on Wiley Online Library for rules of use; OA articles are governed by the applicable Creative Commons License

Accepted Manuscript

[23] P. Rohland, E. Schröter, O. Nolte, G. R. Newkome, M. D. Hager, U. S. Schubert, *Prog. Polym. Sci*. 2022, **125**, 101474.

[24] R. Dantas, C. Ribeiro, M. Souto, *Chem. Commun*. 2024, **60**, 138–149.

[25] J. Bitenc, K. Pirnat, O. Lužanin, R. Dominko, *Chem. Mater*. 2024, **36**, 1025–1040.

[26] N. Goujon, M. Lahnsteiner, D. A. Cerrón-Infantes, H. M. Moura, D. Mantione, M. M. Unterlass, D. Mecerreyes, *Mater. Horiz*. 2023, **10**, 967–976.

[27] T. Wu, Y. Liu, J. Ye, Y. Chen, G. Dai, X. Zhang, Y. Zhao, *J. Power Sources* 2024, **612**, 234779.

[28] W. Xue, H. Mutlu, H. Li, W. Wenzel, P. Theato, *Polym. Chem*. 2021, **12**, 2643–2650.

[29] H. Nishide, S. Iwasa, Y.-J Pu, T. Suga, K. Nakahara, M. Satoh, *Electrochim. Acta* 2004, **50**, 827–831.

[30] C. Liu, X. Huang, X. Yu, Z. Wang, Y. Shen, S. Yuan, Y. Wang, *Angew. Chem. Int. Ed.* 2024, e202415915.

[31] X. Zhou, C. Xu, X. Guo, P. Apostol, A. Vlad, R. A. J. Janssen, S. Er, *Adv. Energy Mater*. 2024, 2401658.

[32] J. T. Liu, E. Grignon, A. M. Battaglia, M. Imran, C. Copeman, H. A. Mills, A. J. Howarth, E. H. Sargent, D. S. Seferos, *Chem. Mater*. 2023, **35**, 9692–9701.

[33] C. Li, X. Liu, Z. He, W. Tao, Y. Zhang, Y. Zhang, Y. Jia, H. Yu, Q. Zeng, D. Wang, J. H. Xin, C. Duan, *J. Power Sources* 2021, **511**, 230464.

[34] H. Wang, C.-J. Yao, H.-J. Nie, K.-Z. Wang, Y.-W. Zhong, P. Chen, S. Mei, Q. Zhang, *J. Mater. Chem. A* 2020, **8**, 11906–11922.

[35] K. Hatakeyama-Sato, S. Matsumoto, H. Takami, T. Nagatsuka, K. Oyaizu, *Macromol. Rapid Commun.* 2021, **42**, 1–7.

[36] S. Wang, A. M. G. Park, P. Flouda, A. D. Easley, F. Li, T. Ma, G. D. Fuchs, J. L. Lutkenhaus, *ChemSusChem* 2020, **13**, 2371–2378.

This article is protected by copyright. All rights reserved.

1864564x, ja, Downloaded from https://chemistry-europe.onlinelibrary.wiley.com/doi/10.1002/cssc.202500092 by A*Star Research Entities, Wiley Online Library on [19/03/2025]. See the Terms and Conditions (https://onlinelibrary.wiley.com/terms-and-conditions) on Wiley Online Library for rules of use; OA articles are governed by the applicable Creative Commons License

Accepted Manuscript

[37] B. Esser, F. Dolhem, M. Becuwe, P. Poizot, A. Vlad, D. Brandell, *J. Power Sources* 2021, **482**, 228814.

[38] T. S. Kim, J. E. Lim, M. S. Oh, J. K. Kim, *J. Power Sources* 2017, **361**, 15–20.

[39] K. Zhang, Y. Hu, L. Wang, J. Fan, M. J. Monteiro, Z. Jia, *Polym. Chem.* 2017, **8**, 1815–1823.

[40] S. Muench, P. Gerlach, R. Burges, M. Strumpf, S. Hoeppener, A. Wild, A. Lex-Balducci, A. Balducci, J. C. Brendel, U. S. Schubert, *ChemSusChem* 2021, **14**, 449–455.

[41] P. Acker, L. Rzesny, C. F. N. Marchiori, C. M. Araujo, B. Esser, *Adv. Funct. Mater.* 2019, **29**, 1906436.

[42] R. Wessling, R. Delgado Andres, I. Morhenn, P. Acker, W. Maftuhin, M. Walter, U. Würfel, B. Esser, *Macromol. Rapid Commun.* 2024, **45**, 2200699.

[43] M. Bhosale, C. Schmidt, P. Penert, G. Studer, B. Esser, *ChemSusChem* 2024, **17**, e202301143.

[44] G. Studer, A. Schmidt, J. Büttner, M. Schmidt, A. Fischer, I. Krossing, B. Esser, *Energy Environ. Sci.* 2023, **16**, 3760–3769.

[45] F. Otteny, M. Kolek, J. Becking, M. Winter, P. Bieker, B. Esser, *Adv. Energy Mater.* 2018, **8**, 1802151.

[46] J. A. Kowalski, M. D. Casselman, A. P. Kaur, J. D. Milshtein, C. F. Elliott, S. Modekrutti, N. H. Attanayake, N. Zhang, S. R. Parkin, C. Risko, F. R. Brushett, S. A. Odom, *J. Mater. Chem. A* 2017, **5**, 24371–24379.

[47] K. A. Narayana, M. D. Casselman, C. F. Elliott, S. Ergun, S. R. Parkin, C. Risko, S. A. Odom, *ChemPhysChem* 2015, **16**, 1179–1189.

[48] Q. Wang, N. Evans, S. M. Zakeeruddin, P. Pechy, I. Exnar, M. Gratzel, *J. Power Sources* 2007, **174**, 408–413.

[49] M. A. Berliner, K. Belecki, *J. Org. Chem*. 2005, **70**, 9618−9621.

This article is protected by copyright. All rights reserved.

1864564x, ja, Downloaded from https://chemistry-europe.onlinelibrary.wiley.com/doi/10.1002/cssc.202500092 by A*Star Research Entities, Wiley Online Library on [19/03/2025]. See the Terms and Conditions (https://onlinelibrary.wiley.com/terms-and-conditions) on Wiley Online Library for rules of use; OA articles are governed by the applicable Creative Commons License

Accepted Manuscript

[50] E. Gitzhofer, B. Vileno, M. Bouquey, D. Chan-Seng, *Polym. Chem.* 2023, **14**, 934–942.

[51] T. D. Lee, J. F. W. Keana, *J. Org. Chem.* 1975, **40**, 3145–3147.

[52] Q. Huang, D. Choi, L. Cosimbescu, J. P. Lemmon, *Phys. Chem. Chem. Phys.* 2013, **15**, 20921–20928.

[53] M. Kolek, F. Otteny, J. Becking, M. Winter, B. Esser, P. Bieker, *Chem. Mater.* 2018, **30**, 6307–6317.

[54] Y. Gong, W. Zhang, Z. Liu, M. Fang, J. Yang, Y. Wang, M. Gao, J. Zhang, Q.-H. Yang, Z. Li, *Adv. Mater.* 2024, **36**, 2312486.

[55] C. L. Berhaut, D. Lemordant, P. Porion, L. Timperman, G. Schmidt, M. Anouti, *RSC Adv*. 2019, **9**, 4599–4608.

[56] P. Gerlach, R. Burges, A. Lex-Balducci, U. S. Schubert, A. Balducci, *J. Power Sources* 2018, **405**, 142–149.

[57] H. Tan, D. Zhai, F. Kang, B. Zhang, *Carbon* 2021, **178**, 363–370.

This article is protected by copyright. All rights reserved.

1864564x, ja, Downloaded from https://chemistry-europe.onlinelibrary.wiley.com/doi/10.1002/cssc.202500092 by A*Star Research Entities, Wiley Online Library on [19/03/2025]. See the Terms and Conditions (https://onlinelibrary.wiley.com/terms-and-conditions) on Wiley Online Library for rules of use; OA articles are governed by the applicable Creative Commons License

Accepted Manuscript